

MICROSCOPIC CALCULATION OF ANTIPIRON NUCLEUS ELASTIC SCATTERING

H.Heiselberg, A.S. Jensen, A.Miranda, G.C. Oades

Institute of Physics, University of Aarhus, DK-8000 Aarhus C, Denmark

and

J.M.Richard

Institute Max von Laue-Paul Langevin, F-38042 Grenoble, France

Elastic scattering cross sections of 300 MeV/c and 600 MeV/c antiprotons on ^{12}C , ^{40}Ca and ^{208}Pb have recently been very accurately measured¹⁾. Microscopic calculations of the antiproton-nucleus optical potential and the related cross sections are available^{2,3,4)}. The results of these calculations are very different according to which method, approximations and basic two-body interaction have been used. In this paper we calculate the antiproton elastic scattering cross section from the Dover-Richard interaction⁵⁾ with a different and simple method which contains the essential ingredients. To study the model and its capabilities, medium corrections are, for the present, ignored.

For a definite isospin I and spin S , the central part of the elastic antiproton-nucleon T-matrix elements corresponding to the Dover-Richard interaction are parametrized by a sum of Yukawas

$$T_C^{IS}(k^2, r) = \sum_{j=1}^{N_C} (a_j (IS) + k^2 b_j (IS)) \exp(-\mu_j r) / (\mu_j r) \quad (1)$$

where k , the CM momentum in fm^{-1} units, is given by

$$k = (ME/2\mu^2)^{1/2} \quad (2)$$

E being the antiproton kinetic energy in the system where the target nucleon is stationary. The coefficients a_j and b_j are determined by making a least squares fit to the Dover-Richard forward scattering amplitude plus s and p-waves over a limited energy range. (For the 300 MeV/c calculations the range $20 \leq E \leq 100$ MeV was used and for the 600 MeV/c calculations $100 \leq E \leq 300$ MeV was used.) In each case the first term in the sum was held fixed at the one pion exchange value (using $\frac{G^2}{4\pi} = 14.43$) and fits were made with 2 and with 3 additional Yukawas. For comparison similar fits were also made with the OPE Yukawa plus 2 or 3 Gaussians.

In order to use this parametrization in a calculation of the optical potential we have to decide how to treat the k^2 term in eq.(1). One possibility is to express k^2

in terms of gradients acting to the left and to the right i.e.

$$k^2 f(r') + -\frac{1}{2} (\hat{\nabla}_{ip}^2 f(r') + f(r') \hat{\nabla}_{ip}^2) \quad (3)$$

where $f(r')$ is any function of $r' = |\mathbf{r} - \mathbf{r}_i|$ and where

$$\hat{\nabla}_{ip}^2 = \frac{1}{2} (\hat{\nabla}_{\mathbf{r}_i} \cdot \hat{\nabla}_{\mathbf{r}'}) = (-\hat{\nabla}_{ip})^2 \quad (4)$$

In this case the central part of the optical potential is given by

$$V_c(r) = \langle \phi | \sum_{i=1}^A [C(|\mathbf{r}_i - \mathbf{r}|) - \frac{1}{2} (\hat{\nabla}_{ip}^2 D(|\mathbf{r}_i - \mathbf{r}|) + D(|\mathbf{r}_i - \mathbf{r}|) \hat{\nabla}_{ip}^2)] | \phi \rangle \quad (5)$$

where $|\phi\rangle$ is the nuclear ground state wave function, where

$$C(r') = \sum_{I,S} \sum_{j=1}^{N_c} a_j(I,S) \exp(-\mu_j r') / (\mu_j r') \quad (6)$$

and where $D(r')$ is given by a similar equation with $a_j(I,S)$ replaced by $b_j(I,S)$. Eq.(5) can be evaluated giving ($r'' = |\mathbf{r}' - \mathbf{r}|$)

$$\begin{aligned} V_c(r) = -\frac{\hat{\nabla}_{\mathbf{r}}}{4} \cdot \frac{1}{4} & \left[[\rho_0(r') G_0(r'') - \rho_1(r') G_1(r'')] d^3 \mathbf{r}' \hat{\nabla}_{\mathbf{r}} + \right. \\ & \left. \int [\rho_0(r') (F_0(r'') - \frac{3}{8} \Delta G_0(r'')) - \rho_1(r') (F_1(r'') - \frac{3}{8} \Delta G_1(r'')) \right. \\ & \left. - \frac{1}{4} (G_0(r'') \tau_0(r') - G_1(r'') \tau_1(r'))] d^3 \mathbf{r}' \right] \end{aligned} \quad (7)$$

where the densities ρ and kinetic densities τ are related to those of the proton and neutron by

$$\rho_0 = \rho_p + \rho_n \quad \rho_1 = \rho_p - \rho_n \quad (8a)$$

$$\tau_0 = \tau_p + \tau_n \quad \tau_1 = \tau_p - \tau_n \quad (8b)$$

The functions F are given by

$$F_0(r'') = \frac{1}{16} \sum_{j=1}^{N_c} [a_j(00) + 3a_j(01) + 3a_j(10) + 9a_j(11)] \exp(-\mu_j r'') / (\mu_j r'') \quad (9a)$$

$$F_1(r'') = \frac{1}{16} \sum_{j=1}^{N_c} [-a_j(00) + a_j(10) - 3a_j(01) + 3a_j(11)] \exp(-\mu_j r'') / (\mu_j r'') \quad (9b)$$

while the functions G are given by corresponding definitions with the a_j 's replaced by b_j 's. (Note that in the case of the Gaussian fits the Yukawas in eqs.(9) must be replaced by Gaussians). In evaluating (5) we have neglected those probability current terms which vanish for time reversal symmetric nuclear wave functions. Using semi-

classical approximations⁶⁾ for τ , the potential is finally expressed in terms of the nuclear density distributions ρ_p and ρ_n and the effective mass in eq.(7) is removed by a suitable transformation of the radial Schrödinger equation leading to an energy dependent optical potential.

Instead of expressing k^2 in terms of gradients, an alternative approach is to approximate it by its average value $\langle k_{ip}^2 \rangle$ obtained from the Fermi motion of the nucleons within the nucleus. The resulting potential can be obtained from eq.(7) by setting $G_0 \approx G_1 \approx 0$ and by replacing $a_j(\text{IS})$ by $a_j(\text{IS}) + \langle k_{ip}^2 \rangle b_j(\text{IS})$ in eqs.(9).

In the calculations the nuclear density distributions are obtained from the charge distribution as measured by electron scattering experiments⁷⁾. In eq.(7) they have to be modified because of the finite size of the antiproton and this is approximately taken care of by making use of the relation⁸⁾

$$\langle r^2 \rangle_p = \langle r^2 \rangle_{\text{ch}} - \langle r^2 \rangle_{\bar{p}} \quad (10)$$

where the subscript p refers to the modified density distribution, ch to the charge distribution and \bar{p} to the finite extension of the antiproton.

The optical potentials for ^{12}C , ^{40}Ca and ^{208}Pb for antiproton momenta of 300 MeV/c and 600 MeV/c are shown in fig.1 for the two alternative treatments of the k^2 terms in eq.(1). In the case where the k^2 terms are replaced by their operator forms, the curves correspond to the potentials after transforming the effective mass terms away. The tail regions are in general quite similar as are the high energy imaginary parts. Otherwise significant differences are apparent. The imaginary depth seems to saturate at about 150 MeV.

In fig.2 we compare the elastic scattering cross sections with the experimental results. The two potentials lead to almost identical cross sections which overall agree remarkably well with the measurements. There is a clear tendency to underestimate the cross sections at larger angles at the high energy.

The other T-matrix approximations also give fairly similar cross sections which can be classified by their χ^2/N -values. With this measure we find that Gaussians in general give worse fits than Yukawa functions. There is no clear preference for either the "gradient" or "average k^2 " treatment.

Changing the neutron density distribution to give a skin thickness⁹⁾ of 0.4 fm for ^{208}Pb leads to a surprisingly small change in χ^2 .

In conclusion the very simple two-body T-matrix approximations and our method of including its energy dependence leads to a satisfactory agreement with elastic scattering cross sections, especially considering the parameter free microscopic nature of our computations. The results of our procedure are described in more detail in a forthcoming publication¹⁰⁾.

REFERENCES

1. D.Garreta et al., Phys.Lett.135B(84)266, 139B(84)464, 149B(84)266 and private communication
2. A.M.Green et al., Nucl.Phys.A377(82)441, A399(83)307, A404(83)495
3. J.Kronenfeld et al. Nucl.Phys.A430(84)525
4. T.Suzuki and N.Narumi, Phys.Lett.125B(83)251, Nucl.Phys.A426(84)413
5. C.Dover and J.M.Richard, Phys.Rev.C21(80)1466
6. M.Brack et al., Phys.Lett.65B(76)1
7. C.W.De Jager et al., Atomic Data and Nuclear Date Tables 14(74)479
8. P.E.Hodgson, "Nuclear Reactions and Nuclear Structure", Oxford University Press, 1971, p.128
9. W.D.Myers and W.J.Swiatecki, Ann.Phys.55(69)395
10. H.Heiselberg et al. University of Aarhus preprint 1985, to be published

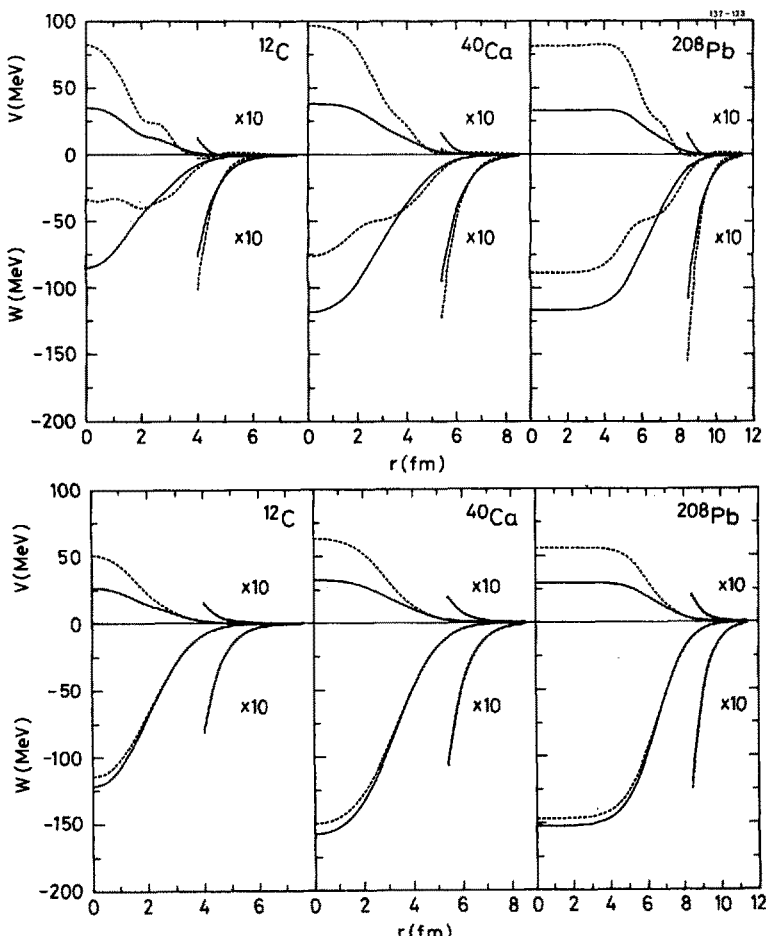


Fig. 1. The real (V) and imaginary (W) part of the optical potential as function of the radius r for various nuclei. All the curves correspond to the T-matrix approximation with three Yukawa functions plus that of the pion. The antiproton momentum is 300 MeV/c in the upper figure and 600 MeV/c in the lower figure. The dashed curves are the potentials corresponding to eq.(7) and the solid curves are those arising from eq.(3) by substituting k_{ip}^2 by its average value $\langle k_{ip}^2 \rangle = 0.75 \text{ fm}^{-2}$. The tail part of the potentials are also shown enlarged by a factor of ten.

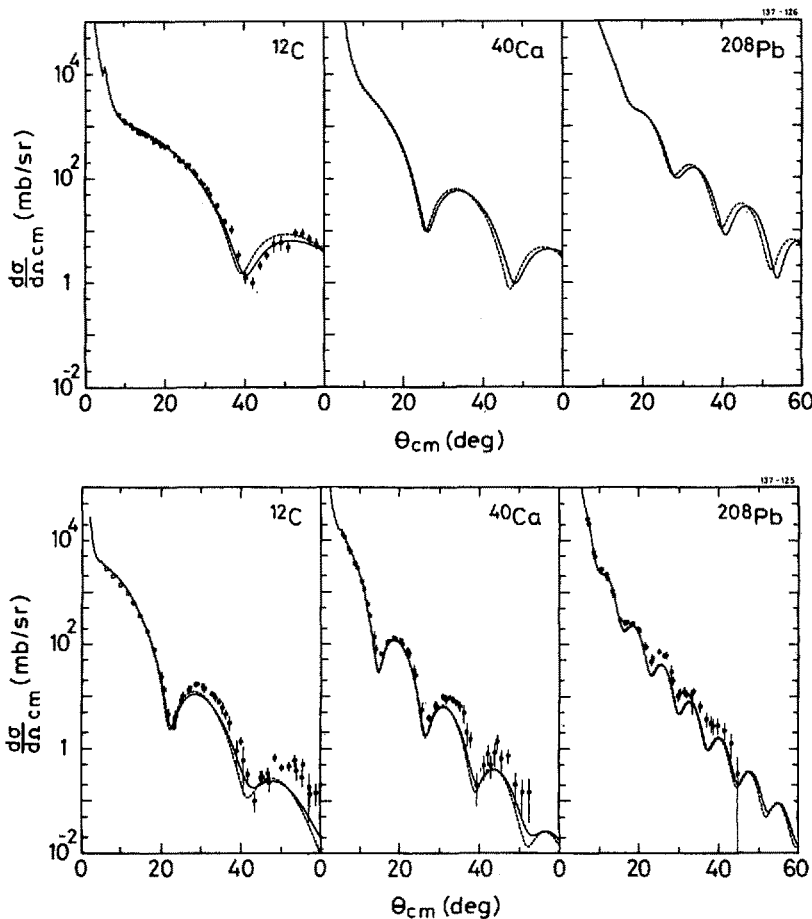


Fig. 2. The differential antiproton-nucleus elastic scattering cross sections as functions of angle for various nuclei. The curves are obtained with the potentials of fig. 1 and the experimental points are from ref.1.